HYDROLOGICAL PROCESSES, VOL. 11, 1427–1439 (1997)

SATELLITE REMOTE SENSING OF RIVER INUNDATION AREA, STAGE, AND DISCHARGE: A REVIEW

LAURENCE C. SMITH[1]

[1]*University of California, Los Angeles, Department of Geography, Los Angeles, CA 90095-1524, U.S.A.*

ABSTRACT

The growing availability of multi-temporal satellite data has increased opportunities for monitoring large rivers from space. A variety of passive and active sensors operating in the visible and microwave range are currently operating, or planned, which can estimate inundation area and delineate flood boundaries. Radar altimeters show great promise for directly measuring stage variation in large rivers. It also appears to be possible to obtain estimates of river discharge from space, using ground measurements and satellite data to construct empirical curves that relate water surface area to discharge. Extrapolation of these curves to ungauged sites may be possible for the special case of braided rivers.

Where clouds, trees and floating vegetation do not obscure the water surface, high-resolution visible/infrared sensors provide good delineation of inundated areas. Synthetic aperture radar (SAR) sensors can penetrate clouds and can also detect standing water through emergent aquatic plants and forest canopies. However, multiple frequencies and polarizations are required for optimal discrimination of various inundated vegetation cover types. Existing single-polarization, fixed-frequency SARs are not sufficient for mapping inundation area in all riverine environments. In the absence of a space-borne multi-parameter SAR, a synergistic approach using single-frequency, fixed-polarization SAR and visible/infrared data will provide the best results over densely vegetated river floodplains. © 1997 John Wiley & Sons, Ltd.

Hydrol. Process., Vol. 11, 1427–1439 (1997)

(No. of Figures: 3 No. of Tables: 0 No. of Refs: 103)

KEY WORDS remote sensing; river inundation; review; synthetic aperture radar, Landsat, floods

INTRODUCTION

Satellite-derived flood inundation maps produced in near-real time are invaluable to state or national agencies for disaster monitoring and relief efforts. New facilities are being developed that will utilize Internet/World Wide Web technology to disseminate satellite data rapidly during flood events (Biasutti and Lombardi, 1995; Blyth 1995). Precise mapping of the maximum flood extent is also required for detecting deficiencies in existing flood control measures and for arbitrating damage claims later.

Remote sensing has proved useful in ecological, hydrological and geomorphological river studies. Its value in remote regions has been demonstrated in the Amazon Basin (Sipple *et al.*, 1992; Koblinsky *et al.*, 1993; Hess *et al.*, 1995), where seasonal to interannual variations in stage and floodplain inundation area are needed for assessing biogeochemical processes such as methane flux and main stem–floodplain exchange (Asselmann and Crutzen, 1989; Richey *et al.*, 1989; Richey *et al.*, 1991). Smith *et al.* (1995a,b) describe a method for using ERS (European Space Agency) high-resolution SAR (synthetic aperture radar) satellite imagery to estimate discharge in remote, braided, glacial rivers that may be sensitive to changing regional or global climate. ERS–SAR data have also been proposed as a source for validation of numerical hydraulic flow models, which predict floodwave surface profiles and inundation patterns (Bates and Anderson, 1995).

Swamp and other habitat types in the large and ecologically diverse Okavango Delta of Botswana have been mapped using Landsat MSS (Ringrose *et al.*, 1988) and TM (Watson, 1991) imagery. A similar study established the morphometry and connectivity of the thousands of channels, lakes and ponds that constitute the Mackenzie Delta in Canada's Northwest Territories (Mouchot *et al.*, 1991); the derived information is useful for watercraft navigation, fisheries and wildlife habitat monitoring. Intermittently flooded areas that

CCC 0885–6087/97/101427–13$17·50

Received 30 October 1995
Accepted 30 April 1996

are potential breeding grounds for mosquitoes that carry the dangerous Rift Valley Fever virus have been mapped in Kenya using Landsat TM and airborne polarimeter data (Pope *et al*., 1992). Floodplain boundaries and land surface types can be delineated with Landsat (Rango *et al*., 1975; Hollyday, 1976; Sollers *et al*., 1978); Nagarajan *et al*. (1993) used Landsat images and aerial photographs over the Rapti River in India to identify areas vulnerable to channel migration and floods.

The sensors used in these and other river studies may be classified into two types: (1) passive, in which the sensor receives energy naturally reflected by or emitted from the earth's surface; and (2) active, in which the sensor provides its own illumination and records the amount of incident energy returned from the imaged surface. Passive sensors include all of the visible and infrared instruments such as the Landsat Thematic Mapper (TM) and Multi-Spectral Scanner (MSS), the Advanced Very High Resolution Radiometer (AVHRR), the Satellite Pour l'Observation de la Terre (SPOT) and the anticipated Advanced Spaceborne Thermal Emission and Reflection Radiometer (ASTER), Moderate-Resolution Imaging Spectroradiometer (MODIS) and Landsat-7 sensors. Passive microwave radiometers such as the Special Sensor Microwave/Imager (SSM/I) measure the amount of microwave energy naturally emitted from the Earth's surface. However, the poor spatial resolution of spaceborne microwave radiometers (*ca*. 27 km at 37 GHz) limits their use to very large areas. This problem has been mitigated through use of spectral mixing models, which extract subpixel proportions of spectrally distinct end members (Sipple *et al*., 1992; Hamilton *et al*., 1996).

The active sensors described in this review consist of imaging radars and radar altimeters. Radars can penetrate clouds, darkness and, at the longer wavelengths, tree canopies. Cloud penetration is particularly important for monitoring flood events, as they commonly occur during periods of extended rainfall. However, interpretation of synthetic aperture radar (SAR) imagery is less straightforward than for the visible/infrared range. In addition, the presence of wind-induced waves or emergent vegetation can roughen the surface of open water bodies, making them difficult to discriminate from other, non-flooded land surface types.

The aim of this paper is to review briefly efforts to use active and passive remote sensing to estimate water surface area, stage and discharge. Methods for mapping surface area are by far the best developed. More recently, improvements in satellite orbital precision and the increasing availability of multi-temporal satellite data have enabled the estimation of river stage and discharge from space. While these techniques are largely in their infancy and not yet used operationally, three general approaches have emerged: (1) direct measurement of water surface level from radar altimeter waveform data; (2) determination of water surface elevations at their point of contact with the land surface using high-resolution satellite imagery and topographic data; and (3) correlation of satellite-derived water surface areas with ground measurements of stage or discharge. It should be noted that river flow velocity cannot be directly measured from space. Satellite estimates of discharge therefore require the use of ground-based empirical relationships between discharge and inundation area or stage.

Studies that have used passive (visible, infrared and microwave range) and active (microwave) sensors to delineate inundation area are reviewed in the first section, and efforts to estimate river stage and discharge from space are reviewed in the second section.

REMOTE SENSING OF INUNDATION AREA WITH PASSIVE AND ACTIVE SENSORS

Visible/infrared Remote Sensing of Inundation Area

Much of the pioneering work on the remote sensing of floods was accomplished using the Multi-Spectral Scanner (MSS) sensor on ERTS-1 (the first Earth Resources Technology Satellite, later renamed Landsat-1), launched on 23 July 1972. With a spatial resolution of about 80 m, MSS data were used to map the extent of flooding in Iowa (Hallberg *et al*., 1973; Rango and Salomonson, 1974), Arizona (Morrison and Cooley, 1973), Virginia (Rango and Salomonson, 1974) and along the Mississippi River (Deutsch *et al*., 1973; Deutsch and Ruggles, 1974; Rango and Anderson, 1974; McGinnis and Rango, 1975; Deutsch, 1976; Morrison and White, 1976). Maximum flood boundaries derived from the MSS imagery were shown to

agree well with those derived from aerial photography (Hallberg *et al*., 1973; Morrison and Cooley, 1973) and US Army Corps of Engineers and US Geological Survey flood hazard maps (Rango and Anderson, 1974). In one case, the MSS-derived flood hazard map performed best, near a major tributary where backwater flooding occurred (Rango and Anderson, 1974). In all studies, MSS band 7 (0·8–1·1 μm) was most useful for discriminating water from dry soil or vegetated surfaces owing to the strong absorption of water in the near-infrared range. This was further confirmed by comparing panchromatic and colour infrared aerial photographs over inundated areas (Hallberg *et al*., 1973; Moore and North, 1974), and by analysing MSS band 5 (0·6–0·7 μm), band 7 and field spectral radiometer data along shoreline water–wet soil–dry soil transitions (Gupta and Banerji, 1985). Errors in MSS-derived flooded areas have been estimated to be less than 5% (Rango and Salomonson, 1974); a similar error estimate has been reported for lakes (Gupta and Banerji, 1985). Chidley and Drayton (1986) suggested that the SPOT system can detect water bodies smaller than 0·5 ha. France and Hedges (1986) found minimum detectable lake areas of 0·6 ha for TM and 2·4 ha for MSS. However, only a 64% accuracy was reported for MSS classifications of flooded land in Bangladesh, where the 80 m spatial resolution failed to resolve adequately the raised dike system that separates rice paddies and serves as infrastructure for transport and dwellings (Imhoff *et al*., 1987). Even larger errors can occur in flooded forests, because trees are highly reflective in the visible and near-infrared range (Hallberg *et al*., 1973; Moore and North, 1974). Floating emergent macrophytes are also a problem in many riverine environments, particularly in tropical systems such as the Amazon (Melack *et al*., 1994; Hess, 1995). Vila da Silva and Kux (1992) noted a significant underestimation of inundation area over such aquatic habitats when using Landsat TM.

Perhaps the greatest problem with visible/infrared sensors is their inability to image the Earth's surface during cloudy conditions (Rango and Salomonson, 1977; Lowry *et al*., 1981; Van den Brink, 1986; Blyth and Biggin, 1993; Rasid and Pramanik, 1993; Melack *et al*., 1994). For the purpose of determining maximum flood extent, this difficulty is somewhat mitigated by the fact that residually wet soils and stressed vegetation can be mapped even after flood stage recession (Rango and Anderson, 1974; Deutsch, 1976). This effect can last from one to two weeks (Hallberg *et al*., 1973; Rango and Salomonson, 1974; Morrison and White, 1976; Salomonson, 1983).

Other studies have continued the methodology first developed with MSS, using TM and SPOT data (France and Hedges, 1986; Jensen *et al*., 1986; Watson, 1991; Blasco *et al*., 1992; Pope *et al*., 1992; Vila da Silva and Kux, 1992). There has also been some success studying very large rivers or floods with the coarser resolution (*ca*. 1 km) US National Ocean and Atmospheric Administration Very High Resolution Radiometer (VHRR) (McGinnis and Rango, 1975; Dey *et al*., 1977), the Advanced Very High Resolution Radiometer (AVHRR) (Ali *et al*., 1989; Barton and Bathols, 1989; Gale and Bainbridge, 1990; Rasid and Pramanik, 1993) and the Nimbus-7 Coastal Zone Color Scanner (CZCS) (Wiesnet and Deutsch, 1987). However, since the 1970s there has been little change in the way visible/infrared satellite data are used to map open water bodies. The approach is relatively straightforward and now considered operational where trees and vegetation do not obscure the water surface and clear skies prevail to permit data acquisition.

Passive Microwave Remote Sensing of Inundation Area

Natural thermal emission of microwaves from the Earth's surface may be measured by passive microwave radiometers such as the Scanning Multichannel Microwave Radiometer (SMMR) which flew on board the Nimbus-7 satellite from 1978 to 1987, and the Special Sensor Microwave/Imager (SSM/I) currently operating on a DMSP (Defense Meteorological Satellite Program) platform. Brightness temperatures (K) measured at the sensor are proportional to the product of the effective surface temperature and the emissivity of the emitting medium (Choudhury, 1989). At the 37 GHz frequency, atmospheric water vapour content and temperature influence the received brightness temperatures. To mitigate these effects, the difference between the vertically and horizontally polarized brightness temperatures (ΔT) is often used instead of the actual brightness temperatures. Large values of ΔT are found over surfaces that emit a strongly polarized microwave signal (such as open water). Depolarization by scattering from vegetation or

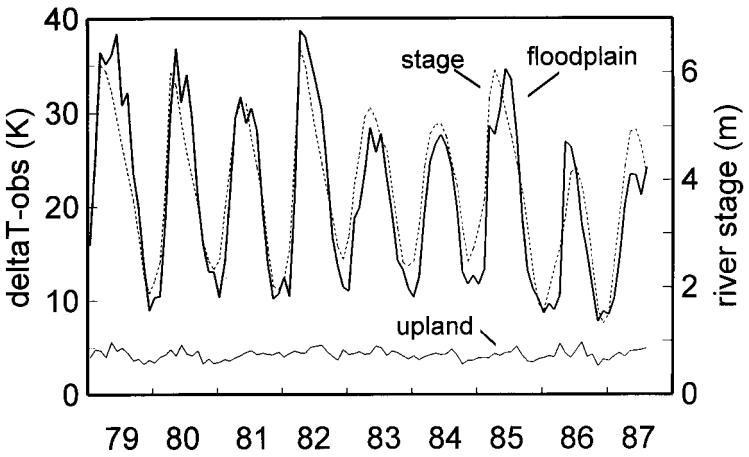

Figure 1. Time trends from 1979 to 1987 of the SMMR 37 GHz polarization difference observed at the satellite (ΔT-obs) over a seasonally inundated Pantanal floodplain (bold solid line) and a nearby upland area (solid line). Polarization difference values are averaged from four SMMR grid cells (floodplain) and sixteen grid cells (upland). Monthly mean stage from the Paraguay River (dashed line) is also shown. The strong correlation between the 37 GHz polarization difference and observed river stage indicate that seasonal differences in ΔT are driven largely by inundation cycles. (From Hamilton *et al.*, 1996)

surface roughness causes values of ΔT to decrease (Schmugge *et al.*, 1986; Choudhury, 1989). Scattering from precipitating clouds can also exert a depolarizing effect, reducing ΔT (Hamilton *et al.*, 1995). A theoretical basis for the use of ΔT over land surfaces is provided by Choudhury (1989). In general, the polarization difference ΔT decreases with increasing vegetation density and surface roughness, and increases over wet or inundated soils.

In South America, monthly SMMR-derived values of ΔT were used to determine seasonal inundation patterns for 15 rivers and wetlands in the Amazon, La Plata, Orinoco and Sáo Francisco river systems (Giddings and Choudhury, 1989; Choudhury, 1991). Distinct differences in the timing of seasonal flow cycles can be seen in the ΔT time-series from a selection of basins, with more subtle differences found among rivers of the same system. These studies were limited to the continental scale by the *ca.* 27 km resolution of SMMR at 37 GHz. An improved 37 GHz resolution of 14 km will be provided by the Multi-Frequency Imaging Microwave Radiometer (MIMR), scheduled for launch on the EOS-PM platform in the year 2000. At present, subpixel estimates of inundation area may be extracted from 37 GHz SMMR data, using empirically derived values of ΔT for open water, seasonally flooded land and non-flooded land as end-member inputs to a linear spectral mixing model (Sipple *et al.*, 1994; Hamilton *et al.*, 1996). In Figure 1, SMMR 37 GHz polarization differences for a seasonally inundated floodplain from the Pantanal wetland of South America are presented with monthly mean ground measurements of discharge in the Paraguay River. Polarization differences for a nearby, non-inundated upland area are also shown. A screening procedure was used to eliminate SMMR images that were affected by heavy rains. Values of ΔT over the inundated floodplain correspond closely with ground measurements of stage in the Paraguay River, the major outlet of the Pantanal. Polarization differences over non-inundated upland show little or no change over time, demonstrating that fluctuations in inundation area are responsible for the corresponding changes in microwave emission from the flooded land surface.

Radar (active microwave) Remote Sensing of Inundation Area

Spaceborne radars can image the Earth's surface in all weather conditions, day or night. As described earlier, the inability of visible/infrared sensors to penetrate clouds poses a severe problem for regular monitoring of river conditions. For example, in the Amazon basin, a search of Landsat data archives from 1972–1985 found just 1–3 useful images per year, most occurring between July and October (Melack *et al.*,

1994). Rasid and Pramanik (1993) cited pervasive cloud cover as the single greatest limitation to their study of flooding in Bangladesh using AVHRR imagery. Van den Brink (1986) reported the same difficulty in Kenya.

An early attempt to map flood inundation extent with active microwaves used a side-looking airborne radar (SLAR) at the X- and L-bands (Lowry *et al*., 1981). X-band SLAR imagery, acquired in the late 1970s was also used to map floodplain lakes along the Amazon River, Brazil (Sipple *et al*., 1992). At the First ERS Thematic Working Group Meeting on Flood Monitoring (ESA/ESRIN, 1995), numerous investigators presented flood inundation maps derived from C-band ERS-1 synthetic aperture radar (SAR) images. A general observation was that for smooth open water bodies without vegetation, especially trees, radar returns are normally low due to specular reflection from the water surface. This characteristic permits flood boundaries to be determined with a good level of accuracy under many conditions. However, turbulence, wind, emergent vegetation and trees can all cause significant increases in radar back-scatter, making inundation extent difficult or impossible to determine.

When a micro-scale element (at the scale of the radar wavelength) of an imaged surface is subjected to an incident microwave, the ratio of incident energy reflected away from the surface to the energy refracted downwards into the media is proportional to the dielectric constant and the incidence angle at which the microwave intersects the imaged surface. The complex dielectric constant of a material is proportional to the strength of its dipole moment in the presence of a time-varying external electric field, while the incidence angle (at the micro-scale) is determined by the surface roughness. Over a larger area (such as a pixel), the angular radiation pattern reflected by the surface is also affected by the local slope, which exerts a net directionality to the radiation pattern. For smooth water bodies, surface roughness and the local slope are both nearly flat. Consequently, most incident microwave energy impacts the surface obliquely and is specularly reflected away from the satellite, yielding low radar returns. Wind reduces this effect by roughening the water surface, increasing radar back-scattering to the satellite. Since water bodies are perfectly saturated, dielectric contrast effects are less important than surface roughness effects. This is not the case for unsaturated soils, where the presence of liquid water causes increased radar back-scatter owing to an increased complex dielectric constant of the soil–water mixture. When the soil becomes saturated and water is ponded, specular reflection is enabled (in the absence of wind or emergent vegetation) and back-scatter to the satellite is dramatically reduced.

Where vegetation or trees are present, a wavelength-dependent increase in radar back-scatter is commonly observed. Surface roughness elements of the order of the radar wavelength exert maximum scattering effect. For example, X-band (2·4–3·8 cm) and C-band (3·8–7·5 cm) signals are effectively scattered by the leaves, twigs and branches within a forest canopy. L-band (15·0–30·0 cm) and P-band (30·0–100·0 cm) display greater canopy penetration but interact strongly with trunks and large branches. Radar impulses are transmitted and received in plane-polarized form by the radar antenna. Polarizations may be transmitted and received horizontally (HH), vertically (VV) or cross-polarized (HV or VH). Radars with multiple frequencies and polarizations provide much more information about the imaged surface than single-polarization, fixed-frequency radars. L-band radar back-scatter is commonly increased over flooded forests through a double-bounce mechanism between the water surface and inundated tree trunks or branches (Hoffer *et al*., 1985; Harris and Digby-Argus, 1986; Richards *et al*., 1987; Hess *et al*., 1990; Hess and Melack, 1994). An HV phase difference of 153° was found in airborne polarimeter data over a forested swamp (Durden *et al*., 1989), agreeing closely with a phase difference of 152° modelled for the site (a pure double-bounce return is defined as having a 180° phase difference between the vertical and horizontal polarizations). The magnitude of the back-scatter increase is significantly affected by vegetation type (Krohn *et al*., 1983; Evans *et al*., 1986; Harris and Digby-Argus, 1986; Pope *et al*., 1994) and may be suppressed altogether by a dense undergrowth between the tree canopy and water surface (Waite *et al*., 1981). Airborne multi-polarization radar studies have generally indicated that flooding beneath forest canopies is best detected with co-polarizations rather than cross-polarizations (Wedler and Kessler, 1981; Hoffer *et al*., 1985; Evans *et al*., 1986; Pope *et al*., 1992; Hess *et al*., 1995), although Wu and Sader (1987) favour use of a co- and cross-polarization ratio.

From L-HH Shuttle Imaging Radar B (SIR-B) SAR data collected over the Altamaha River in Georgia, Hess and Melack (1994) confirmed the observation of Hoffer *et al.* (1985) that L-band enhancement is affected by radar incidence angle. Flooded pine forest could be discriminated from dry forest at incidence angles of 18° and 45° from vertical, but not 58°. Horizontally polarized (HH) C-, L-, and P-band NASA/JPL AIRSAR data were also acquired over this site, and illustrate superbly the features that can be observed in wetlands and flooded forests with different frequencies. Increased returns at C-band over marshes were interpreted as double-bounce reflections between emergent plant stalks and a smooth water surface. These stalk dimensions were too small to increase returns at L- and P-band, so marshes appeared dark at these longer wavelengths. The converse was true in flooded bottomland forests, where L- and P-bands penetrated the upper canopy but experienced double-bounce reflections between the water surface and inundated tree trunks. C-band was attenuated by the leaves and twigs of the forest canopy, except in areas defoliated by caterpillar damage and permanent inundation by beaver ponds (Hess and Melack, 1994). Comprehensive reviews of the interaction of various radars with a wide range of flooded vegetation types are provided by Hess *et al.* (1990) and Melack *et al.* (1994).

Recent efforts have used fully polarimetric SAR data to classify various inundated land surface types. Amplitudes at multiple frequencies and polarizations vary with vegetation structure and species. Multi-parameter SAR can thus be used to detect flooding in vegetated riverine environments to an extent not possible with single-frequency, fixed-polarization radars. Pope *et al.* (1994) presented four biophysical indices that can be used to discriminate thickets and areas of forest regrowth, marshes, swamp forests and upland forests. Hess *et al.* (1994, 1995) used a decision-tree model to classify polarimetric SIR-C (Shuttle Imaging Radar C) acquired over the Negro and Amazon rivers near Manaus, Brazil in April and October, 1994. Both C- and L-bands were used to distinguish open water, floating macrophytes and flooded forest from upland forest and clearings. While the total area of open water did not change significantly between data acquisitions, the extent of flooded forest was nearly 50% less in October. It is clear that multi-parameter SAR offers a distinct advantage over single-frequency, fixed-polarization SAR where diverse vegetation cover is found.

REMOTE SENSING OF RIVER STAGE AND DISCHARGE

In the previous section studies that used passive or active sensors to measure river inundation area or flood extent were reviewed. In this section, a small group of studies that attempted to use satellite data to estimate river stage or discharge are discussed. Such efforts will likely become more common in the future as satellite orbital errors decrease and high-resolution multi-temporal data become more plentiful. Data availability has already increased with the launch of the ERS-1, ERS-2, JERS-1 and RADARSAT spaceborne SARs, which are not limited by weather conditions or darkness. Even more data are anticipated from future high-resolution SARs (JERS-2, ENVISAT-1, RADARSAT-2) and visible/infrared sensors (Landsat-7, ASTER, SPOT 5 and 6).

Radar Altimetry of Water Surface Elevation

Radar altimetry has emerged as a promising method for directly measuring stage variations in large rivers. Radar altimeters emit a short, nadir-directed radar pulse to the Earth's surface. The two-way return time is used to calculate the range between the satellite and the target. Because the pulse is in the form of a curved wave front, a time-varying waveform is returned to the satellite. An on-board tracker, which assumes a gradually changing surface (i.e. ice sheets and water bodies), is used to estimate when the return echo will arrive. Interactions with the surface cause the waveform to be distorted. If the tracker receives a rapidly changing echo, the tracker may not 'lock' properly and range estimates are lost. For this reason, radar altimeters generally do not work well over land. However, where a lock on the land power return is maintained, it is possible to identify peaks in the waveform data that result from specular returns over large rivers (Guzkowska *et al.*, 1990). These spikes progress through the waveform as the satellite passes over the

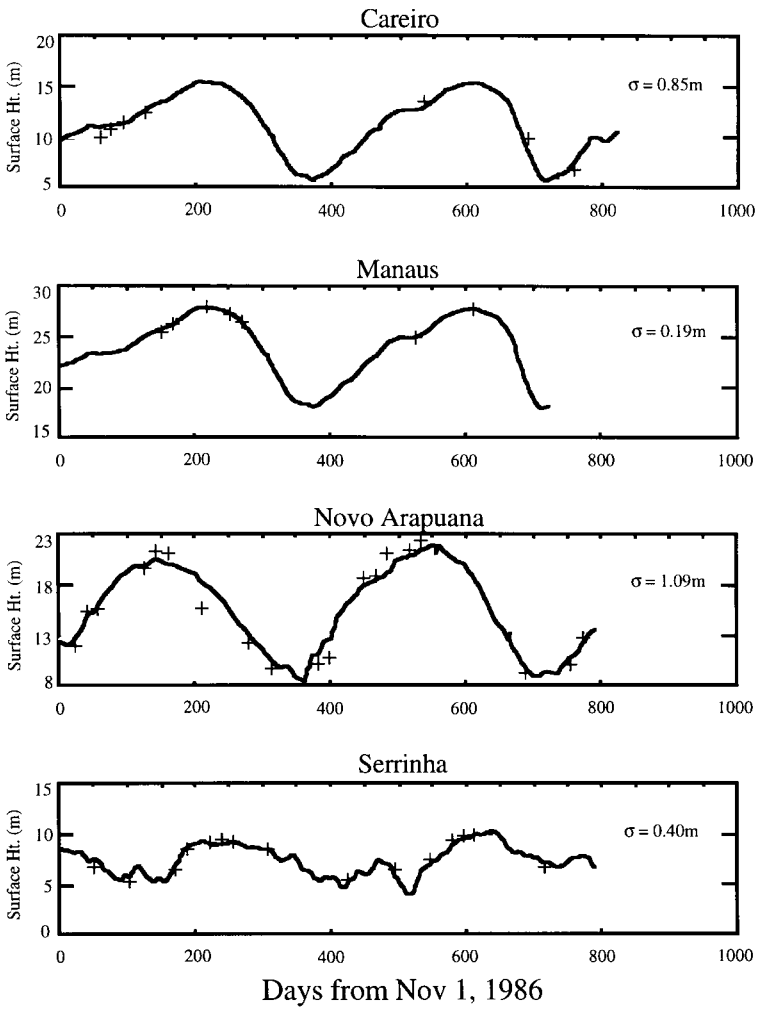

Figure 2. Comparisons in river stage at four sites in the Amazon basin, as estimated from river gauges (solid line) and Geosat altimeter waveforms (pluses). Standard deviations of the differences between the altimeter and river stage data are also shown. Period of observation is from November 1986 to November 1988. (Adapted from Koblinsky *et al.*, 1993)

river. Koblinsky *et al.* (1993) used this approach with Geosat waveform data to estimate river stage at four sites along the Amazon. The derived water surface levels are presented with the corresponding ground measurements in Figure 2. Altimeter ranges were calculated by manually selecting specular returns from the waveform data. An average root mean square error of 0·7 m was found between the ground and altimeter estimates of water surface level. Uncertainties in the ground stage measurements (*ca.* 10 cm or more) and the radial component of the satellite orbit (estimated at 50 cm) were major contributors to this error.

Birkett (1994) obtained lake level changes using a similar analysis of Geosat altimeter waveforms. Her results suggest that radar altimetry can be used to measure relative water level changes in lakes within 10 cm. For very large lakes, waveform analysis is not required to obtain good estimates of water level: Morris and Gill (1994) used average height estimates from the Geosat altimeter to estimate levels in the five Great Lakes of the United States, with an average root mean square error of 11·1 cm. Average heights are a standard altimeter product and represent the average water level over the altimeter footprint, which typically has a radius of several kilometres.

Errors in orbital precision pose the greatest problem to using satellite altimetry to measure stage in rivers or lakes. The Geosat orbital error has been estimated at about 50 cm (Koblinsky *et al*., 1993), although it has been subsequently reduced through recomputation of some of the 17-day exact repeat mission (ERM) orbits (Morris and Gill, 1994). However, this problem is steadily diminishing as satellite tracking systems improve. The radial component of the ERS-1 orbit is determined to within 15 cm; the equivalent error is only 3 cm for TOPEX/Poseidon (Le Traon *et al*., 1995). ERS-1 orbital errors have been reduced even further by using TOPEX/Poseidon data to minimize the variation in measured sea surface heights at points where the two satellite tracks cross (Le Traon *et al*., 1995). As altimeters with small orbital errors (such as TOPEX/Poseidon) become more common, radar altimetry over inland water surfaces may become routine for those sites where a lock on the land surface can be maintained.

Water–surface Elevations from Satellite Imagery and Topographic Data

River stage can be estimated at the land–water contact, using high-resolution satellite imagery in combination with topographic maps or a digital elevation model (DEM). Requirements for this approach are high image and topographic resolution and an unobscured water edge boundary along an area of gently sloping relief. Gupta and Banerji (1985) used topographic maps and Landsat MSS data to obtain water surface elevations for a large reservoir in India. Land–water contact elevations were chosen along two low-gradient, inundated stream channels near their confluences with the reservoir. The derived water surface elevations agreed closely with values estimated from measurements surveyed on the ground.

Miller (1986) used Landsat MSS and 1 : 50 000 topographic maps to obtain spot water surface elevations over the Belize River in Central America. Flood volumes subsequently estimated by assuming mean inundation depths of 1·5–3·0 m were in general agreement with volumes calculated from hydrograph analysis. However, significant parts of the land–water boundary were obscured by vegetation, limiting the spot elevations to areas near permanent lagoons. Brakenridge *et al*. (1994) used ERS-1 SAR images and 1 : 24 000 US Geological Survey topographic maps to pick water edge elevations at gently sloping alluvial fans along the Mississippi River during the 'Great Flood' of 1993. Instantaneous flood stages differed by as much as 2·4 m at opposite sides of the Mississippi River, illustrating the value of this approach for estimating flood profiles and monitoring flood wave dynamics.

Correlation of Inundated Area with Ground Measurements of Stage or Discharge

A third method for estimating river stage or discharge from space is by correlating ground measurements of these variables with satellite-derived estimates of inundation area. Until recently, the major obstacle to this approach has been the requirement of a large number of satellite images to construct empirical rating curves relating inundation area to stage or discharge. Kruus *et al*. (1981) compared total inundation areas from seven Landsat MSS scenes over the St John River in New Brunswick, Canada with simultaneous measurements of river stage. They found a general increase of stage with inundation area, but at some times an increase in stage was associated with a decrease in inundation area. Usachev (1983) used a similar approach to determine the relationship between inundation area and ground measurements of stage and discharge in the Ob River of Siberia. In all of the Ob River analyses, increasing stage or discharge was associated with increasing inundation area. The correlation was quasi-linear and quite similar for three study sections at Mogochin, Kolpashevo and Kargasok. Xia *et al*. (1983) presented a strongly linear correlation between water surface area and ground measurements of water level for Dongting Lake, China's second largest freshwater body.

Until additional empirical rating curves relating inundation area to ground measurements of stage or discharge are made, it is difficult to assess their potential for extrapolation to other rivers of similar morphology. However, it seems likely that such curves will vary significantly between rivers and therefore must be constructed for each site. An exception may be the special case of braided rivers, which display an extreme spatial sensitivity of water surface area to changing discharge, and also share some common morphological properties. Smith *et al*. (1995) used multi-temporal ERS-1 SAR data and simultaneous

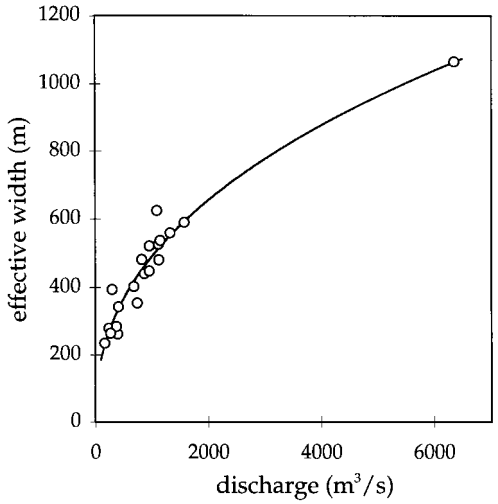

Figure 3. Relationship between satellite-derived effective width and river discharge for a large braided river in Canada. Effective width is the total water surface area contained within a 10 km × 3 km river reach, divided by the reach length. Each point is determined from a single ERS-1 SAR image and a ground measurement of discharge. The outlier is an extreme flood event; maximum annual flows do not normally exceed 2000 m^3/s. (From Smith *et al.*, 1995)

ground measurements of discharge to derive a stable, power-law correlation between satellite-derived water surface area and discharge for a large braided river in Canada (Figure 3). Subsequent work (Smith *et al.*, 1996) found similar curves for two other braided rivers in Alaska and Canada. A theoretical power-law correlation between water surface area and discharge was also found (Smith *et al.*, 1996), using a cellular model of stream braiding (Murray and Paola, 1994). Moderate differences in the satellite-derived rating curves relating water surface area to discharge are explained primarily by the intensity of braiding, with braid channel morphology and valley slope exerting smaller effects. In the absence of ground data, it appears that this method can be used to estimate relative discharge in order to determine the shape and timing of seasonal hydrographs in braided rivers. Absolute discharge can be estimated within a factor of two, with more accurate estimates requiring one or more ground measurements of discharge acquired simultaneously with a satellite image acquisition. More work is needed to determine if known morphological controls, such as total sinuosity, valley slope, bank material and stability, and braid channel hydraulic geometry, can be used to parameterize empirically derived rating curves for extrapolation to other ungauged braided rivers.

CONCLUSIONS

High-resolution visible/infrared sensors such as Landsat provide good delineation of flood extent where clouds, trees or floating vegetation do not obscure the water surface. Passive microwave radiometers show promise for acquiring estimates of inundation area over very large rivers or wetlands, but sensor resolution is coarse and the land–water boundary cannot be located accurately. Spaceborne synthetic aperture radars (SARs) are not limited by weather conditions or darkness. Single polarization, C-band SARs are effective for mapping smooth, open water bodies. However, emergent vegetation, trees, wind or flow turbulence can all increase radar back-scatter returns, making delineation of inundated areas problematic. L-band SARs can penetrate forest canopies and often display increased returns over flooded forest produced by a double-bounce mechanism between inundated tree trunks and the water surface. Multi-frequency polarimetric SAR provides much more information and can be used to classify different types of inundated terrain to an extent not possible with single-frequency SARs and visible/infrared sensors. However, there are no current plans to launch a multi-frequency, fully polarimetric SAR on a satellite platform. As a consequence, a synergistic

remote sensing approach utilizing both visible/infrared and SAR data may be the only effective way to monitor inundation area in vegetated riverine environments. Visible/infrared data will provide good discrimination of flood extent in open areas, identify places where vegetation is a problem and help with interpretation of SAR data. SARs will provide excellent temporal coverage and, in certain situations, will be able to determine the flood extent through emergent plants and forest canopies.

As satellite orbital precision and data availability improve, promising methods for estimating river stage and discharge should continue to develop. Radar altimetry shows potential for measuring stage in large rivers to within 10 cm. Orbital laser altimeters such as GLAS (Geoscience Laser Altimeter System), planned for launch in 2003, should also permit monitoring of stage variation in large rivers. Landsat and ERS-1 SAR data have been combined with topography to obtain water surface elevations at the point of contact between water and land. This approach can also be used to determine lateral asymmetries in river stage and estimate the flood profile. Satellite-derived estimates of water surface area have been correlated with ground measurements of stage or discharge to obtain rating curves that can subsequently be used to estimate these flow variables from satellite data alone. Transfer of such empirical rating curves to estimate discharge in ungauged basins appears feasible in the special case of braided rivers, which are spatially sensitive to changing discharge and commonly share some morphological similarities between sites.

ACKNOWLEDGEMENTS

This work was carried out at the Department of Geological Sciences, Cornell University, with funding from NASA through Graduate Student Researchers Program Fellowship NGT-51223, Mission to Planet Earth/Earth Observing System (EOS) grant NAGW-2638 and Spaceborne Imaging Radar (SIR-C) grant 958745. Helpful comments and assistance were provided by A. Bloom, B. Isacks, J. Liebeskind and R. Forster of the Department of Geological Sciences, Cornell University. S. Hamilton of the W.K. Biological Station, Michigan State University, and C. Koblinsky of NASA/Goddard Space Flight Center provided Figures 1 and 2.

REFERENCES

Ali, A., Quadir, D. A., and Huh, O. K. 1989. 'Study of river flood hydrology in Bangladesh with AVHRR data', *Int. J. Remote Sens.*, **10**(12), 1873–1891.

Asselmann, I. and Crutzen, P. J. 1989. 'Global distribution of natural freshwater wetlands and rice paddies, their net primary productivity, seasonality, and possible methane emissions', *J. Atmos. Chem.*, **8**, 307–358.

Astaras, T. 1985. 'Drainage network analysis of Landsat images of the Olympus-Pieria mountain area, Northern Greece', *Int. J. Remote Sens.*, **6**, 673–686.

Astaras, T., Lambrinos, N., and Soulakellis, N. 1990. 'A drainage system analysis evaluation of, and comparison between, Landsat-3 RBV, Landsat-5 TM and SPOT PA imageries covering the Central Macedonia district, Greece', *Int. J. Remote Sens.*, **11**(9), 1549–1559.

Barrett, E. C., Herschy, R. W., and Stewart, J. B. 1988. 'Satellite remote sensing requirements for hydrology and water management from the mid 1990's, in relation to the Columbus Programme of the European Space Agency', *Hydrol. Sci. J.*, **33**(1), 1–17.

Barton, I. J., and Bathols, J. M. 1989. 'Monitoring floods with AVHRR', *Remote Sens. Environ.*, **30**, 89–94.

Bates, P. D. and Anderson, M. G. 1995. 'Issues of hydraulic model validation and design using remotely sensed data', *Proceedings, First ERS Thematic Working Group Meeting on Flood Monitoring*, European Space Agency/ESRIN, Frascati, Italy, 26–27 June 1995.

Bhavsar, P. 1984. 'Review of remote sensing applications in hydrology and water resources management in India', *Adv. Space Res.*, **4**(11), 193–200.

Biasutti, R. and Lombardi, A. 1995. 'EARTHWATCH: a service provided by EURIMAGE — the flood case', *Proceedings, First ERS Thematic Working Group Meeting on Flood Monitoring*, European Space Agency/ESRIN, Frascati, Italy, 26–27 June 1995.

Birkett, C. M. 1994. 'Radar altimetry: a new concept in monitoring lake level changes', *EOS Trans., AGU*, **75**(24), 273–275.

Blasco, F., Bellan M. F., and Chaudhury, M. U. 1992. 'Estimating the extent of floods in Bangladesh using SPOT data', *Remote Sens. Environ.*, **39**, 167–178.

Blyth, K. 1995. 'FLOODNET — a telenetwork for acquisition, processing, and dissemination of Earth Observation data for monitoring and emergency management of floods', *Proceedings, First ERS Thematic Working Group Meeting on Flood Monitoring*, European Space Agency/ESRIN, Frascati, Italy, 26–27 June 1995.

Blyth, K. and Biggin, D. S. 1993. 'Monitoring floodwater inundation with ERS-1 SAR', *Earth Obs. Quart.*, **42**, 6–8.

Brakenridge, G. R., Knox, J. C., Paylor, E. D., and Magilligan, F. J. 1994. 'Radar remote sensing aids study of the great flood of 1993', *EOS Trans., AGU*, **75**(45), 521–527.

Brooner, W. G. and Binaghi, C. M. V. 1983. 'Landsat monitoring of temporal hydrological variations on the Pilcomayo River, 1972–1981', *Proceedings, 17th International Symposium on Remote Sensing of the Environment*., Ann Arbor, MI, pp. 399–407.

Chidley, T. R. E. and Drayton, R. S. 1986. 'The use of SPOT-simulated imagery in hydrological mapping', *Int. J. Remote Sens.*, **7**(6), 791–799.

Choudhury, B. J. 1989. 'Monitoring global land surface using Nimbus-7 37 GHz data: theory and examples', *Int. J. Remote Sens.*, **10**(10), 1579–1605.

Choudhury, B. J. 1991. 'Passive microwave remote sensing contribution to hydrological variables', *Surv. Geophys.*, **12**, 63–84.

Cihlar, J., Pultz, T. J., and Gray, A. L. 1992. 'Change detection with synthetic aperture radar', *Int. J. Remote Sens.*, **13**(3), 401–414.

Deutsch, M. 1976. 'Optical processing of ERTS data for determining extent of the 1973 Mississippi River flood', *U.S. Geol. Surv. Prof. Pap. 929*, ERTS-1, a New Window on Our Planet, pp. 209–222.

Deutsch, M. and Ruggles, F. 1974. 'Optical data processing and projected applications of the ERTS-1 imagery covering the 1973 Mississippi River Valley floods', *Wat. Resour. Bull.*, **10**(5), 1023–1039.

Deutsch, M., Ruggles, F. H., Guss, P., and Yost, E. 1973. 'Mapping of the 1973 Mississippi river floods from the Earth Resources Technology Satellite', *Proceedings, International Symposium on Remote Sensing and Water Resources Management*, American Water Resources Association, Proceedings no. 17, Burlington, Ontario, pp. 39–55.

Dey, B., Moore, H., and Gregory, A. F. 1977. 'The use of satellite imagery for monitoring ice break-up along the Mackenzie River, N.W.T', *Arctic*, **30**(4), 234–242.

Durden, S. L., Van Zyl, J. J., and Zebker, H. A. 1989. 'Modeling and observation of the radar polarization signature of forested areas', *IEEE Trans. Geosci. Remote Sens.*, **27**(3), 290–301.

ESA/ESRIN, 1995. *First ERS thematic Working Group Meeting on Flood Monitoring*, Frascati, Italy, 26–27 June 1995.

Evans, D. L., Farr, T. G., Ford, J. P., Thompson, T. W., and Werner, C. L. 1986. 'Multipolarization radar images for geologic mapping and vegetation discrimination', *IEEE Trans. Geosci. Remote Sens.*, **GE-24**(2), 246–257.

Ferguson, H. L., Deutsch, M., and Kruus, J. 1980. 'Applications to floods of remote sensing from satellites', *Adv. Space Res.*, **9**, 195–206.

France, M. J. and Hedges, P. D. 1986. 'A hydrological comparison of Landsat TM, Landsat MSS, and black and white aerial photography', in Damen, Smit, and Verstappen (Eds), *Proceedings, 7th International Symposium, ISPRS (Internat. Soc. Photogram. and Remote Sens.) Commission VII*, Enschede, 25–29 August 1986, pp. 717–720.

Gale, S. J. and Bainbridge, S. 1990. 'The floods in eastern Australia', *Nature*, **345**, 767.

Giddings, L. and Choudhury, B. J. 1989. 'Observation of hydrological features with Nimbus-7 37 GHz data, applied to South America', *Int. J. Remote Sens.*, **10**(10), 1673–1686.

Gupta, R. P. and Banerji, S. 1985. 'Monitoring of reservoir volume using Landsat data', *J. Hydrol.*, **77**, 159–170.

Gupta, R. P. and Bodechtel, J. 1982. 'Geotechnical applications of Landsat image analysis of Bhakra dam reservoir, India', *Remote Sens. Environ.*, **12**, 3–13.

Guzkowska, M. A. J., Rapley, C. G., Ridley, J. K., Cudlip, W., Birkett, C. M., and Scott, R. F. 1990. 'Developments in inland water and land altimetry', *European Space Agency Contract Report 7839/88/F/FL*.

Hallberg, G. R., Hoyer B. E., and Rango, A. 1973. 'Application of ERTS-1 imagery to flood inundation mapping', *NASA Special Pub. No. 327*, Symposium on significant results obtained from the Earth Resources Satellite-1, Vol. 1, Technical presentations, section A, pp. 745–753.

Hamilton, S. K., Sipple, S. J., and Melack, J. M. 1996. 'Inundation patterns in the Pantanal wetland of South America determined from passive microwave remote sensing.' *Arch. Hydrobiol.*, **137**, 115–141.

Harris, J. and Digby-Arbus, S. 1986. 'The detection of wetlands on radar imagery', *Proceedings, 10th Canadian Remote Sensing Symposiums* Edmonton, Alberta, 5–8 May, 1986. Canadian Aeronautics and Space Institute, Ottawa, pp. 529–543.

Hess, L. L. and Melack, J. M. 1994. 'Mapping wetland hydrology and vegetation with synthetic aperture radar', *Int. J. Ecol. Environ. Sci.*, **20**, 197–205.

Hess, L. L., Melack, J. M., and Simonett, D. S. 1990. 'Radar detection of flooding beneath the forest canopy: a review', *Int. J. Remote Sens.*, **11**(7), 1313–1325.

Hess, L. L., Melack, J. M., and Davis, F. W. 1995. 'Mapping of floodplain inundation with multi-frequency polarimetric SAR: use of a tree-based model', *Proceedings of the 1994 Int. Geosci. and Remote Sens. Symp* (IGARSS '94), pp. 1072–1073.

Hess, L. L., Melack, J. M., Filoso, S., and Wang, Y. 1995. 'Delineation of inundated area and vegetation along the Amazon floodplain with the SIR-C synthetic aperture radar', *IEEE Trans. Geosci. Remote Sens.*, **33**(4), 895–903.

Hockey, B., Richards, T., and Osmaston, H. 1990. 'Prospects for operational remote sensing of surface water', *Remote Sens. Rev.*, **4**(2), 265–283.

Hoffer, R. M., Mueller, P. W., and Lozano-Garcia, D. F. 1985. 'Multiple incidence angle shuttle imaging radar data for discriminating forest cover types', *Proceedings, ASCM-ASPRS Fall Technical Meeting*, Indianapolis, 8–13 September 1985, pp. 476–485.

Hollyday, E. F. 1976. 'Improving estimates of streamflow characteristics by using Landsat-1 imagery', *J. Res. US Geol. Surv.*, **4**(5), 517–531.

Imhoff, M. and Gesch, D. 1988. 'The derivation of sub-canopy surface terrain models of coastal forests using synthetic aperture radar', *Proceedings, 1988 Int. Geosci. and Remote Sens. Symp* (IGARSS '88), pp. 613–617.

Imhoff, M. L., Vermillion, C., Story, M. H., Choudhury, A. M., Gafoor, A., and Polcyn, F. 1987. 'Monsoon flood boundary delineation and damage assessment using space borne imaging radar and Landsat data', *Photogramm. Eng. Remote Sens.*, **53**(4), 405–413.

Jensen, J. R., Hodgson, M. E., Christensen, E., Mackey, H. E., Jr., Tinney, L. R., and Sharitz, R. 1986. 'Remote sensing inland wetlands: a multispectral approach', *Photogramm. Eng. Remote Sens.*, **52**, 87–100.

Koblinsky, C. J., Clarke, R. T., Brenner, A. C., and Frey, H. 1993. 'Measurement of river level variations with satellite altimetry', *Wat. Resour. Res.*, **29**(6), 1839–1848.

Krohn, M. D., Milton, N. M., and Segal, D. B. 1983. 'Seasat synthetic aperture radar (SAR) response to lowland vegetation types in eastern Maryland and Virginia', *J. Geophys. Res.*, **88**(C3), 1937–1952.

Kruus, J., Deutsch, M., Hansen, P. L., and Ferguson, H. L. 1981. 'Flood applications of satellite imagery' in *Satellite Hydrology, Proceedings, Fifth Ann. William T. Pecora Memorial Symp. on Remote Sens., 1979*, Amer. Wat. Resour. Assoc. Tech. Pub. No. TPS 81–1, pp. 292–301.

Le Traon, P. Y., Gaspar, P., Ogor, F., and Dorandeu, J. 1995. 'Satellites work in tandem to improve accuracy of data', *EOS Trans., AGU,* **76**(39), 385–389.

Lowry, R. T., Langham, E. J., and Mudry, N. 1981. 'A preliminary analysis of SAR mapping of the Manitoba Flood, May 1979', in *Satellite Hydrology, Proceedings, Fifth Ann. William T. Pecora Memorial Symp. on Remote Sens., 1979*, Amer. Wat. Resour. Assoc. Tech. Pub. No. TPS81-1, pp. 316–323.

Macdonald, H. C., Waite, W. P., and Demarcke, J. S. 1980. 'Use of Seasat satellite radar imagery for the detection of standing water beneath forest vegetation', *Tech. Papers of the Amer. Soc. of Photogramm. Fall Tech. Meeting*, Niagara Falls, New York, 7–10 October, 1980, RS3B1–RS3Bl3.

McGinnis, D. F. and Rango, A. 1975. 'Earth Resources Satellite systems for flood monitoring', *Geophys. Res. Let.*, **2**(4), 132–135.

Melack, J. M., Hess, L. L., and Sippel, S. 1994. 'Remote sensing of Lakes and Floodplains in the Amazon Basin', *Remote Sens. Rev.,* **10**, 127–142.

Mertes, L. A. K., Smith, M. O., and Adams, J. B. 1993. 'Estimating suspended sediment concentrations in surface waters of the Amazon River wetlands from Landsat images', *Remote Sens. Environ.*, **43**, 281–301.

Miller, S. T. 1986. 'The quantification of floodplain inundation by the use of Landsat and metric camera information, Belize, Central America', *Proceedings, 7th International Symposium, ISPRS (Internat. Society Photogrammetry and Remote Sensing) Commission VII*, Enschede August 1986, pp. 733–738.

Moore, G. K. and North, G. W. 1974. 'Flood inundation in the southeastern United States from aircraft and satellite imagery', *Wat. Resour. Bull.*, **10**(5), 1082–1096.

Morris, C. S. and Gill, S. K. 1994. 'Variation of Great Lakes water levels derived from Geosat altimetry', *Wat. Resour. Res.*, **30**(4), 1009–1017.

Morrison, R. B. and Cooley, M. E. 1973. 'Assessment of flood damage in Arizona by means of ERTS-1 imagery', *Proceedings, Symposium on Significant Results Obtained from the Earth Resources Satellite-1*, Vol. 1, New Carrollton, Maryland, pp. 755–760.

Morrison, R. B. and White, P. G. 1976. 'Monitoring flood inundation', *U.S. Geol. Surv. Prof. Pap. 929*, ERTS-1, A New Window on Our Planet, pp. 196–208.

Mouchot, M. C., Alfoldi, T., DeLisle, D., and McCullough, G. 1991. 'Monitoring the water bodies of the Mackenzie Delta by remote sensing methods', *Arctic,* **44** (suppl. 1), 21–28.

Muller, E., Décamps, H., and Dobson, M. K. 1993. 'Contribution of space remote sensing to river studies', *Freshwater Biol.*, **29**, 301–312.

Murray, A. B. and Paola, C. 1994 'A cellular model of braided rivers', *Nature,* **371**, 54–57.

Nagarajan, R., Marathe, G. T., and Collins, W. G. 1993. 'Identification of flood prone regions of Rapti river using temporal remotely-sensed data', *Int. J. Remote Sens.*, **14**(7), 1297–1303.

Ormsby, J. P., Blanchard, B. J., and Blanchard, A. J. 1985. 'Detection of lowland flooding using active microwave systems', *Photogramm. Eng. Remote Sens.*, **51**(3), 317–328.

Philipson, W. R. and Hafker, W. R. 1981. 'Manual versus digital Landsat analysis for delineating river flooding', *Photogramm. Eng. Remote Sens.*, **47**(9), 1351–1356.

Pope, K. O., Sheffner, E. J., Linthicum, K. J., Bailey, C. L., Logan, T. M., Kasichke, E. S., Birney, K., Njogu, A. R., and Roberts, C. R. 1992. 'Identification of Central Kenyan Rift Valley Fever virus vector habitats with Landsat TM and evaluation of their flooding status with airbourne imaging radar', *Remote Sens. Environ.*, **40**, 185–196.

Pope, K. O., Rey-Benayas, J. M., and Paris, J. F. 1994. 'Radar remote sensing of forest and wetland ecosystems in the Central American tropics', *Remote Sen. Envion.*, **48**, 205–219.

Rango, A. and Anderson, A. T. 1974. 'Flood hazard studies in the Mississippi River basin using remote sensing', *Wat. Resour. Bull.*, **10**(5), 1060–1081.

Rango, A. and Salomonson, V. V. 1973. 'Repetitive ERTS-1 observations of surface water variability along rivers and low-lying areas', *Amer. Wat. Resour. Assoc. Proc. no. 17*, Remote Sensing and Water Resources Management, pp. 191–199.

Rango, A. and Salomonson, V. V. 1974. 'Regional flood mapping from space', *Wat. Resour. Res.*, **10**(3), 473–484.

Rango, A. and Salomonson, V. V. 1977. 'The utility of short wavelength (< 1 mm) remote sensing techniques for the monitoring and assessment of hydrological parameters' *Proceedings, 11th Int. Symp. on Remote Sens. of Environ.*, Ann Arbor, MI, 25–29 April 1977, pp. 55–64.

Rango, A., Foster, J., and Salomonson, V. V. 1975. 'Extraction and utilization of space acquired physiographic data for water resources development', *Wat. Resour. Bull,* **11**(6), 1245–1255.

Rapley, C. G., Baker, S. G., Birkett, C. M., Laxon, S. W., Ridley, J. K., Scott, R. F., and Strawbridge, F. 1992. 'ERS-1 altimetry of inland water and land', *Proceedings, First ERS-1 Symp., ESA SP-359 (March, 1993)*, Cannes, France, 4–6 November, 1992, pp. 539–542.

Rasid, H. and Pramanik, M. A. H. 1993. 'Areal extent of the 1988 flood in Bangladesh: how much did the satellite imagery show?', *Natural Hazards*, **8**, 189–200.

Rast, M., Jaskolla, F., and Arnason, K. 1991. 'Comparative digital analysis of Seasat-SAR and Landsat-TM data for Iceland', *Int. J. Remote Sens.*, **12**(3), 527–544.

Richards, J. A., Sun, G.-Q., and Simonett, D. S. 1987a. 'L-band radar backscatter modeling of forest stands', *IEEE Trans. Geosci. Remote Sens.*, **25**, 487–498.

Richards, J. A., Woodgate, P. W., and Skidmore, A. K. 1987b. 'An explanation of enhanced radar backscattering from flooded forests', *Int. J. Remote Sens.*, **8**(7), 1093–1100.

Richey, J. E., Mertes, L. A. K., Dunne, T., Victoria, R. L., Forsberg, B. R., Tancredi, A., and Oliveira, E. 1989. ' Sources and routing of the Amazon River flood wave', *Global Biogeochem. Cycles*, **3**, 1991–204.

Richey, J. E., Victoria, R. L., Salati, E., and Forsberg, B. R. 1991. 'The biogeochemistry of a major river system: the Amazon case study', in Degens, E. T., Kempe, S., and Richey, J. E. (eds), *Biogeochemistry of Major World Rivers*, John Wiley & Sons, Ltd, Chichester. pp. 57–74.

Ringrose, S., Matheson, W., and Boyle, T. 1988. 'Differentiation of ecological zones in the Okavango Delta, Botswana, by classification and contextural analysis of Landsat MSS data', *Photogramm. Eng. Remote Sens.*, **54**(5), 601–608.

Salomonson, V. V. (Ed.), 1983. 'Water resources assessment', in *Manual of Remote Sensing*, Chap. 29, Amer. Soc. of Photogramm. pp. 1497–1570.

Salomonson, V. V. and Rango, A. 1974. 'ERTS-1 applications in hydrology and water resources', *J. Amer. Wat. Works Assoc.*, **66**(3), 168–172.

Schmugge, T. 1987. 'Remote sensing applications in hydrology', *Rev. Geophys.*, **25**(2), 148–152.

Schmugge, T. J., O'Neill, P. E., and Wang, J. R. 1986. 'Passive microwave soil moisture research', *IEEE Trans. Geosci. Remote Sens.*, **24**, 12–22.

Schultz, G. A. 1988. 'Remote sensing in hydrology', *J. Hydrol.*, **100**, 239–265.

Sipple, S. J., Hamilton, S. K., and Melack, J. M. 1992. 'Inundation area and morphometry of lakes on the Amazon River floodplain, Brazil', *Arch. Hydrobiol.*, **123**(4), 385–400.

Sipple, S. J., Hamilton, S. K., Melack, J. M., and Choudhury, B. J. 1994. 'Determination of inundation area in the Amazon River floodplain using the SMMR 37 GHz polarization difference', *Remote Sens. Environ.*, **48**, 70–76.

Smith, L., Isacks, B. L., Forster, R. R., Bloom, A. L., and Preuss, I. 1995. 'Estimation of discharge from braided glacial rivers using ERS-1 SAR: first results', *Wat. Resour. Res.*, **31**, 1325–1329.

Smith, L. C., Isacks, B. L., Bloom, A. L., and Murray, A. B. 1996. 'Estimation of discharge from three braided rivers using synthetic aperture radar (SAR) satellite imagery: potential for application to ungaged basins', *Water Resour. Res.*, **32**(7), 2021–2034.

Sollers, S. C., Rango, A., and Henninger, D. L. 1978. 'Selecting reconnaissance strategies for floodplain surveys', *Wat. Resour. Bull.*, **14**(2), 359–373.

Solomon, S. I. 1992. 'Methodological considerations for use of ERS-1 imagery for the delineation of river networks in tropical forest areas', *Proceedings, First ERS-1 Symp., ESA SP-359 (March, 1993)*, Cannes, France, 4–6 November, 1992, pp. 595–600.

Usachev, V. F. 1983. 'Evaluation of flood plain inundations by remote sensing methods', *Proceedings of the Hamburg Symposium, IAHS Publ., 145*, 475–482.

Van den Brink, J. W. 1986. 'A study with NOAA-7 AVHRR imagery in monitoring ephemeral streams in the lower catchment area of the Tana River, Kenya', Damen, Smit, and Verstappen (Eds.), *Proceedings, 7th International Symposium, ISPRS (Internat. Soc. Photogram. and Remote Sens.) Commission VII*, Enschede, 25–29 August 1986, pp. 783–785.

Van Es, E., Bomez, H., and Soeters, R. 1975. 'An inundation study of the lower Magdalena-Cauca River Basin', *NASA Tech. Memo X-58168*, Vol. 1-D, pp. 2295–2297.

Vila da Silva, J. S. and Kux, H. J. H. 1992. 'Thematic mapper and GIS data integration to evaluate the flooding dynamics within the Panatal, Mato Grosso do Sul State, Brazil', *Proceedings, 1992 Int. Geosci. Remote Sens. Symp.* (IGARSS '92), pp. 1478–1480.

Waite, W. P., MacDonald, H. C., Kaupp, V. H., and Demarcke, J. S. 1981. 'Wetland mapping with imaging radar', *Proceedings, 1981 Int. Geosci. and Remote Sens. Symp.* (IGARSS '81), pp. 794–799.

Watson, J. P. 1991. 'A visual interpretation of a Landsat mosaic of the Okavango Delta and surrounding area', *Remote Sens. Environ.*, **35**, 1–9.

Wedler, E. and Kessler, R. 1981. 'Interpretation of vegetative cover in wetlands using four-channel SAR imagery', *Tech. Papers of the Amer. Soc. of Photogramm.*, ASP-ASCM Convention, Washington, D.C., 22–27 February, 1981, pp. 111–124.

Whitelaw, A., Howes, S., Fletcher, P. and Rast, M. 1995. 'Remote sensing applications in hydrological modelling', *SPIE* (*Soc. of Photo-Optical Instrumentation Engineers*) vol. 2314, *Multispectral and Microwave Sensing of Forestry, Hydrology, and Natural Resources*, Rome, Italy, 26–30 September, 1994, pp. 618–627.

Wiesnet, D. R. and Deutsch, M. 1987. 'Flood monitoring in South America from the Landsat NOAA and NIMBUS Satellites', *Adv. Space Res.*, **7**(3), 77–84.

Wu, S. T. and Sader, S. A. 1987. 'Multipolarization SAR data for surface feature delineation and forest vegetation characterization', *IEEE Trans. Geosci. Remote Sens.*, **GE-25**(1), 67–76.

Xia, Liu, Shulin, Z., and Xianglian, L. 1983. 'The application of Landsat imagery in the surveying of water resources of Dongting Lake', *Proceedings of the Hamburg Symposium, IAHS Publ.*, **145**, 483–489.

